Secondary-electron emission from porous solids

Jean M. Millet
Laboratoire d'Astronomie Spatiale, ERS CNRS 81, Traverse du Siphon, Les Trois Lucs, Boîte Postale 8, 13376 Marseille Cedex 12, France

Jean-Pierre J. Lafon
Observatoire de Paris, DASGAL/URA CNRS D0335, 92195 Meudon Cedex, France
(Received 18 October 1993; revised manuscript received 27 September 1994)

Porous structure can strongly change the electric behavior of material submitted to bombardment by energetic electrons: strong electric fields (10^8 V/m) can grow within the pores, because of the small sizes of these pores. We give a model of porous material that enables us to emphasize and illustrate the enhancement of the yield of secondary-electron emission (and the broadening in frequency of its profile) in a porous medium, compared to that in bulk material. Here we have considered materials of astrophysical interest [graphite, iron, aluminum (Al_2O_3), and silica]. The enhancement is characterized by two emission peaks for small energies of the primary electrons and by an increase of the yield roughly by a factor of 4 for large energies (> 1 keV).

PACS number(s): 79.20.Hx, 96.50.Dj, 95.30.Qd

I. INTRODUCTION

Secondary electron emission (hereafter denoted by SEE) follows from energy exchange between the so-called "primary" electrons, striking the material, and the electrons inside the material, resulting in so called "secondary" electrons, expelled out of the material. Primary electrons with energies lower than a few hundred eV are quickly absorbed: they cannot travel along distances larger than a few angstroms, while excited electrons easily escape. Now, at larger energies, electrons are excited more deeply inside the material so that it is more difficult for them to escape; this is obvious in Fig. 1, which shows the yield of the SEE versus the energy of incident electrons. Thus, one can expect that, for porous materials, in which holes and pieces of material with different scale sizes are mixed, the yield of the SEE is certainly greatly changed.

For porous layers of MgO, Jacobs, Freely, and Brandt [1] measured yields higher than those of bulk material by a factor 100, suggesting that this could be due to a discharge following the growth of strong electric fields throughout the pores. Millet and Lafon [2–4], used this model to describe the behavior of probably porous dust grains [5,6] in astrophysical plasmas.

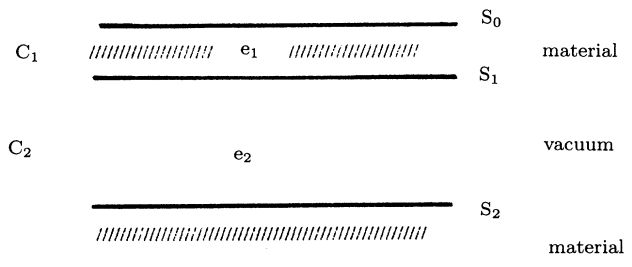

FIG. 1. Yield of secondary electron emission (in emitted electron per incident electron) for carbon, iron, silica, and aluminum (Al_2O_3) versus the energy of the incident electron, for bulk materials.

In Sec II of this paper, we summarize the model of Jacobs, Freely, and Brandt and the results already obtained with it [3] under astrophysical conditions, emphasizing the relations between the stimulated electric field and the yield of secondary electron emission; then (Sec. III) we describe the SEE produced [7] inside a bulk material in which the penetration of an electron and the absorption of its energy can be described using the Whiddington law. This is used in Sec. IV to describe a simple model of porous material with which the behavior of dust grains in astrophysical plasmas was already outlined elsewhere [4], and for which we now analyze the coefficient of SEE (Sec. V). Sections VI and VII are respectively devoted to numerical results obtained with the model and to the discussion and the conclusions.

II. MODEL OF JACOBS, FREELY, AND BRANDT

The very high SEE yields measured from insulators under peculiar physical conditions were quickly attributed to the growth of strong electric fields inside the material: a synthetic view of various analyses was given by McKay [7].

However, Jacobs and co-workers [1,8,9] were the first authors to show by experiment the link between these phenomena and the porosity of the material. Layers of MgO were obtained by deposition of magnesium under an oxygen pressure of 80 μm and then oxidation by inductive heating under 2 mm of oxygen [1]. This method was responsible for the porous structure of the MgO layers.

With a microscope, one can observe a uniform distribution of small 6-μm-high and 2-μm-thick stalactites. The nonporous layers exhibit more spherical and less uni-

form small structures. The mean thickness of the layers analyzed is 1 μm and the currents of the primaries range between 1 and 10 μA with electron energies below 400 eV. Under such conditions, the bulk material on which the layers are deposited seems to play no role, since all the primary electrons are confined to the porous layer. Besides, the SEE is highly sensitive to the strength of the electric field in front of the layer (with an exponential dependence); it looks to be independent of the energy of the primary electrons.

All these results led Jacobs, Freely, and Brandt to analyze the emission mechanism in terms of field emission analogous to the Townsend discharge in gases; then the emitted current J was related to the incident current J_p as

$$\delta = J/J_p = \exp(\alpha x_m) ,$$

where x_m and α, respectively, denote the penetration depth inside the material and the number of excited electrons per incident electron and unit length; these parameters are related to the pressure p, the mean-free path L_e, the electric field E, and the extraction potential V_i through the equation of von Engel and Steenberg [1]

$$\alpha = \frac{2.4\times 10^3}{\pi} p L_e \left[1+\frac{16V_i}{2\pi^2 L_e E}\right] \exp\left[\frac{-16V_i}{\pi^2 L_e E}\right] .$$

For weak enough fields E, α is proportional to E,

$$\alpha = \chi E, \quad \text{with } \chi = 0.059 V^{-1} \text{ for MgO} .$$

The strength of the electric field E is determined by the boundary conditions on the surface together with Ohm's law

$$E = J_p(\delta-1)\rho[1-\exp(-t/\rho\varepsilon)] ,$$

where ρ and ε respectively denote the resistivity and the permittivity of the material. It is obvious from this equation that the electric field grows in the porous layer with a characteristic growth time equal to $\rho\varepsilon$, say 10^{-5} s for MgO.

From all these equations one can derive an equation relating the value of δ and that of the primary current, in the steady state:

$$\ln\delta/(\delta-1) = J_p \rho e x_m \chi .$$

Millet, Lafon, and Gonin [3] used this model to compute the floating potential of porous grains embedded in astrophysical plasmas, but in a way suitable for grains with lower sizes (the typical grain sizes do not exceed 100 μm).

The porosity of the grains was inferred from the polarization and the forward scattering of the light crossing interplanetary or interstellar dust clouds [6]; observations of dust grains collected in the terrestrial atmosphere support such an hypothesis [5]. The pores should be micrometer sized. Assuming that grains grow by continuous collection of gas particles [10] or by electrostatic attraction of small grains of different sizes and materials [11,12], one can imagine that porosity does not only occur close to the surface but exists inside the material with many small cavities.

In the experiments of Jacobs and co-workers, the primary electrons with small energy (say below 300 eV) cannot cross the stalactites and reach the deeper layers through free paths, they generate additional secondaries in other stalactites. We describe a model of porous material with holes separated by walls of bulk material in which the primaries must cross some layers of bulk material before reaching empty pores to generate secondary electrons. Thus, the range of energy of the efficient primary electrons is fairly higher than that involved in the experiments of Jacobs and co-workers, since, for instance, crossing a layer of 0.1 μm of silica requires energies greater than 1000 eV. Consequently, our mechanism is somewhat different from that described by Jacobs and co-workers, both by the energy of the primary electrons and the way in which they interact with matter. It will be efficient in hot plasmas (for instance, in some planetary magnetospheres), or when dust grains are submitted to cosmic rays; this is the subject of a forthcoming paper.

III. MECHANISM OF SECONDARY-ELECTRON EMISSION

The energy of an electron with initial energy E_0 penetrating into bulk material at a distance x from the surface is given by Whiddington law (13)

$$E^2(x) = -bx + E_0^2 ,$$

assuming normal incidence; this assumption will be used throughout the sequel. The coefficient b was derived by Bohr [14,15] for β rays and cathodic rays:

$$b = 4\pi e^4 N L ,$$

where e is the electron charge, N the atomic number, and L an average (dimensioned) logarithmic term weakly sensitive to the mean rotation frequency of any bound electron. For iron, $b = 9.784\times 10^{-24}$ kg^2 m^3 sec^{-4}. The maximum penetration length is $x_m = E_0^2/b$. For electrons with an energy of 1000 eV incident on iron, $x_m = 2.617\times 10^{-9}$ m. Let dJ_s denote the current of secondary electrons generated in a slab dx at a distance x from the surface by the primary current J_p,

$$dJ_s = -KJ_p(dE(x)/dx)\exp(-kx)dx , \tag{1}$$

where K^{-1} is the energy released and carried away by the ejected electron:

$$dE(x)/dx = -b/2E(x) = -b/[2(E_0^2-bx)^{1/2}] , \tag{2}$$

according to Whiddington's law; k is the absorption coefficient and $\exp(-kx)$ is a probability for a primary electron at distance x from the surface to generate a secondary electron. The minus sign expresses the decrease of the electron energy inside the material. In the case of slabs of bulk material with thickness e_1 large enough, i.e., when $E_0^2 < be_1$, the yield of secondary emission is given by

$$\delta(E_0) = J_s/J_p = \frac{Kb}{2}\int_0^{E_0^2/b} (E_0^2-bx)^{-1/2}\exp(-kx)dx , \tag{3}$$

TABLE I. Values for various materials.

Material	Density cm^{-3}	δ_m	$10^{24}b$ ($kg^2\,m^3sec^{-4}$)	E_m eV	K^{-1} eV	$k=\alpha^{-1}$ ($10^8\ m^{-1}$)
Graphite	2.26	1	1.432	250	117	7.575
S_iO_2	2.65	2.9	2.143	420	67.9	4.016
Mica	2.8	2.4	1.061	340	66.1	3.036
Iron	7.86	1.3	5.377	400	144	11.11
Al	2.70	0.95	1.8394	300	147	6.757
MgO	3.58	23	4.668	1200	24.3	1.071
Lunar dust	3.2	1.5	2.74	500	155	3.623

which can easily be written

$$\delta(E_0)=K(b/k)^{1/2}\exp(-kE_0^2/b)\int_0^{E_0(k/b)^{1/2}}\exp(Y^2)dY\ . \tag{4}$$

In fact, due to their nature b and k are not independent; they characterize, respectively, the energy transport and the probability of electron transfer; now, since the function

$$f(r)=\exp(-r^2)\int_0^r\exp(Y^2)dY$$

has a maximum for $r=0.92$, one can prove that [7]

$$0.92=(k/b)^{1/2}E_{0m}\ , \tag{5}$$

which relates the ratio k/b and the experimental values of E_{0m}.

Table I displays values for various materials (from Draine and Salpeter [17]); thus, for iron, $k=1/(9\times10^{-10})\ m^{-1}$, which, from Eq. (5) with $E_{0m}=400$ eV, leads to $b=5.377\times10^{-24}\ kg^2m^3\,s^{-4}$; this is in fairly good agreement with what can be found using Bohr's formula, in spite of all the simplifying assumptions, so that hereafter we go on using formula (4).

Figure 1 shows the values δ obtained from Eq. (3) versus E_0 for several materials. It is noticeable that the values of δ_m and E_{0m} are on average 25% higher than those of Table I, which were measured values. This is a consequence of the influence on measured collected currents due to the state of the surface, the way in which it was designed, and also the experimental conditions (incidence, vacuum quality, temperature). Another source of discrepancy is the use of Whiddington's law even for very small energies; the main drawback of a law of this type is that, whereas the rate of secondary electron production decreases when the incident energy decreases, which is realistic, it increases to infinity as $E(x)$ decreases to zero [Eqs. (1) and (2)]. Young [16] obtained a better agreement between theoretical and experimental values with an exponent of 1.35 instead of 2. Nevertheless, Whiddington's law leads to much easier and explicit derivations with not strongly different results, so that hereafter we keep to it.

IV. A SIMPLE MODEL OF POROUS MATERIAL

The most realistic way in our opinion to describe the secondary electron emission by porous grains with sizes smaller than 100 μm is to say that the primary electrons must cross a first layer of material, then reach holes where a high electric field will help them to produce other secondary electrons so that the net yield is highly increased.

The easiest way to describe such a phenomenon is to consider a thin layer C_1 of material of thickness e_1 separated from the remaining part of the dust grain by a vacuum layer C_2 of thickness e_2 (Fig. 2). Both e_1 and e_2 are much smaller than the grain size (0.001–0.01 μm $\ll$ 100 μm); one can deal with a problem in plane geometry.

S_0, S_1, and S_2, respectively, denote the outside boundary of the grain, the inside boundary of the outer layer C_1, and the inside boundary of C_2. Crossing C_1, a primary electron generates secondary electrons and progressively loses its energy; if $E_0^2>be_1$ it penetrates into the vacuum pore with an energy E_1, such that

$$E_1^2=E_0^2-be_1\ ,$$

and travels on towards S_2, which bounds bulk material. The secondary emission yield $\delta(E)$ on S_2 is given by Eq. (3). The electrical equilibrium within the bulk material requires, on the surface S_2, a net current equal to zero; in other words,

$$J_p-J_s=J_p-J_p\delta(E)=0\ \text{ so that }\ \delta(E)=1\ . \tag{6}$$

Figure 1 shows that there are two energies $E_l<E_{0m}$ and $E_h>E_{0m}$ satisfying this condition. If $E_1>E_h$, $\delta<1$, and the primary electrons accumulate on the surface S_2,

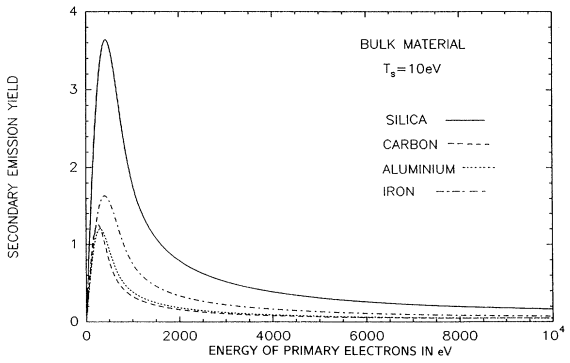

FIG. 2. Illustration of our model of porous medium (details in the text).

S_2 is then negatively charged, which generates an electric field reducing the energy of the primary electrons down to E_h.

If $E_l < E_1 < E_h$, then $\delta > 1$ and the current leaving S_2 is greater than that reaching it; in a transient phase, S_2 acquires a positive charge that increases the energy of the primary electrons towards E_h, and the potential difference $V_2 - V_1$ increases and impedes the ejection of secondary electrons. These leave S_2 with the energy $E_S = k_B T_S$ (k_B is Boltzmann's constant and T_S the mean temperature of emitted secondary electrons). If $E_{1S} = E_S - e(V_2 - V_1) > 0$, they reach S_1 with the energy E_{1S}. Now, since $E_1 - E_h = e(V_1 - V_2)$ (conservation of energy), the condition $E_{1S} > 0$ implies

$$E_1 > E_h - E_S \ . \tag{7}$$

This condition is not much different from the condition $E_1 > E_h$, since E_S (1–10 eV, depending on the material) is always much lower than E_h (a few hundred eV). If $E_{1S} < 0$, i.e., if condition (7) is not satisfied the potential difference $V_2 - V_1$ increases during the transient phase until the secondary electrons emitted from S_2 can never reach S_1 and accelerated primary electrons accumulate on S_2. The only possible equilibrium now becomes that in which a braking electric field decelerates the primary electrons in such a way that they reach the surface S_2, with the energy E_l, and that the net current is zero. This electric field accelerates all the electrons emitted from S_2 to S_1, these electrons reach S_1 with the energy $E_{1S} > 0$ with

$$E_{1S} = E_S - e(V_2 - V_1) = E_S + E_1 - E_l \ . \tag{8}$$

This singular behavior comes from the assumption of a unique velocity for all incident electrons and should be smoothed out by taking into account a full velocity distribution function.

Finally, if $E_1 < E_l$, again $\delta < 1$, the primary electrons accumulate on the surface S_2; S_2 is then negatively charged, which generates an electric field, reducing the energy of the primary electrons until all primary electrons are reflected just on the surface S_2 with no emission of secondary electrons. To summarize:

(i) If $E_1 > E_h$, i.e.,

$$E_0^2 > be_1 + E_h^2 \ ,$$

there is an equilibrium with an electric field directed from S_1 to S_2, which can reach very high values; $e(V_1 - V_2) = E_1 - E_h$.

(ii) Under the condition $E_h - E_s < E_1 < E_h$, i.e.,

$$be_1 + (E_h - E_S)^2 < E_0^2 < be_1 + E_h^2 \ ,$$

there is an equilibrium state with an electric field smaller than E_s/e and directed from S_2 to S_1. Again $e(V_1 - V_2) = E_1 - E_h$.

(iii) Under the condition $E_1 < E_h - E_S$, at equilibrium, there is an electric field directed from S_1 to S_2; $e(V_1 - V_2) = E_1 - E_l$.

(iv) If $E_1 < E_l$, at equilibrium, there is an electric field directed from S_1 to S_2 and $E_1 = e(V_1 - V_2)$.

Under the astrophysical conditions considered (hot planetary magnetospheres and flows of cosmic rays), the most probable case is the first one.

V. ON THE YIELD OF SECONDARY-ELECTRON EMISSION IN POROUS MEDIA

In porous media the electric current pattern is much more complex than in bulk material. The currents can have various sources. Under the conditions of our model, they can be due to electrons emitted in the layer S_1, primary electrons reflected inside the pore between S_1 and S_2 and generating new secondary electrons between S_0 and S_1, and secondary electrons emitted from S_2 and crossing the pore and in turn generating new secondary electrons between S_0 and S_1. In all cases it is assumed that the electron current is constant as long as the energy of the concerned electrons is not zero, whereas electrons that have lost all their energy can be ignored.

If $E_0^2 < be_1$, the primary electrons do not cross the external layer of material and produce a secondary-electron current equal to $J_p \delta(E_0)$.

If $E_0^2 > be_1$, the secondary-electron current stimulated in the outer layer of material is equal to

$$J_{S1} = K(b/k)^{1/2} J_p \exp(-kE_0^2/b) \int_{E_1(k/b)^{1/2}}^{E_0(k/b)^{1/2}} \exp(Y^2) dY \ , \tag{9}$$

the spatial range of integration extending from 0 to e_1 instead of from 0 to x_m. Now, if $E_0^2 > be_1$, one must add the current J_{S2} due to the secondary electrons generated in the bulk material between S_0 and S_1 by the secondary electrons emitted from S_2 or the primary electrons dynamically reflected in the pore. Depending on their energy, the electrons coming from the pore can cross the outer layer of material or not; let E_2 denote this energy. Depending on the four cases distinguished in Sec. IV,

$$E_2 = E_1 - E_h + E_S \quad \text{in cases 1 and 2} \ ,$$

$$E_2 = E_1 - E_l + E_S \quad \text{in case 3} \ ,$$

$$E_2 = E_1 \quad \text{in case 4} \ .$$

If $E_2^2 > be_1$,

$$J_{S2}^0 = K(b/k)^{1/2} J_p \exp\{-k[e_1 - (E_2^2/b)]\} \int_0^{E_2(k/b)^{1/2}} \exp(-Y^2) dY \ , \tag{10}$$

and the primary current J_p flows out of the material. If $E_2^2 < be_1$,

$$J_{S2}^0 = K(b/k)^{1/2} J_p \exp\{-k[e_1 - (E_2^2/b)]\} \int_{(k/b)^{1/2}(E_2^2 - be_1)^{1/2}}^{E_2(k/b)^{1/2}} \exp(-Y^2) dY \ . \tag{11}$$

In all cases the net yield δ is equal to the ratio of the sum of the currents leaving the surface S_0 to the current J_p due to electrons impinging on it.

VI. NUMERICAL RESULTS AND DISCUSSION

We especially investigated porous materials of astrophysical interest made of silica, graphite, iron, and aluminum (in fact, Al_2O_3). However, the features of the yield curve are general and independent of the material, since they mainly result from the model of porous media and the (universal) shape of the yield curve for bulk media.

We computed the net yield of secondary-electron emission δ as a function of the energy of the incident primary electrons, the thickness e_1 of the outer layer, and the average temperature of emission T_S. The computations were performed using a FORTRAN program on an IBM personal computer. The energy of incident primary electrons E_0 ranges between 100 and 10 000 eV in order to mimic plasmas of hot planetary magnetospheres and flows of cosmic rays.

Figure 1 shows the classical curve illustrating the variations of δ versus E_0 for bulk materials (graphite, iron, aluminum, and silica), for which the energy of the primary electrons is completely absorbed. This is the case for the range of energies considered, for $e_1 > 0.1$ μm.

For porous materials ($e_1 < 0.01$ μm), the most obvious result is that δ is roughly higher by a factor 4 for high energies, while it takes its classical values for bulk materials for very small energies or as soon as $e_1 = 1$ μm. Moreover, two peaks with increased yield appear. Compare Figs. 2 and 3; for small energies and values of e_1 lower than 0.1 μm, two peaks appear for silica at energies depending on the temperature (Fig. 3) and the thickness (Fig. 4); for $e_1 > 0.1$ μm, there is only one peak on the figure, the other one appearing for an energy out of the range considered (Fig. 5); this is also the case for the other materials at $e_1 = 0.01$ μm (Fig. 5). Variations of T_S only produce a small linear shift of the energy scale.

Let us now discuss the shape of the yield curve; in particular the peaks. Figure 4 shows the shape of the peaks for $T_S = 10$ eV, depending on the values of e_1. For $e_1 = 0.001$ μm the first peak starts with strong discrepancies from the characteristics of bulk material, for an energy of primary electrons $E_0^0 = 289$ eV ($< E_l$), which corresponds to zero energy at the surface S_1 for an electron crossing the layer C_1; a small increase of E_0 from this value decreases the production rate of secondary electrons [Eq. (1)] and so decreases the secondary current generated in C_1 [the integrand decreases as $(E_0^2 - be_1)^{-0.5}$ and the integration range is unchanged, so that the emission reaches a limit]. Obviously, the greater e_1, the greater the energy $E_0^0 < E_l$, the smaller the alteration of the production rate of secondary electrons close to E_0^0 (the discrepancy is reduced for larger thicknesses e_1).

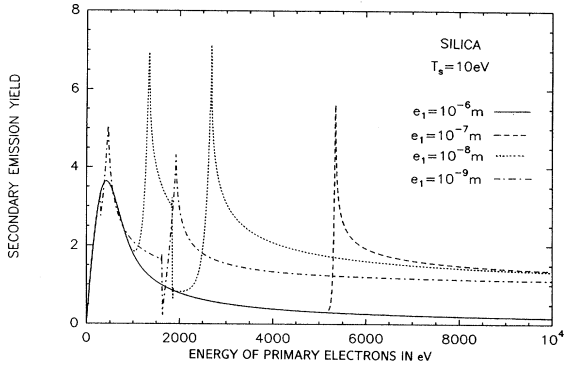

FIG. 4. Yield of secondary electron emission for silica versus the energy of the incident electron, for porous materials, depending on the thickness e_1 of the external layer of material.

For values of E_0 greater than E_0^0, an electric field appears and reflects the incident electrons. The secondary current through C_1 is then increased by the amount of the reflected current and increases. E_1 becomes equal to E_l for $E_0 = 297$ eV.

For $E_0 > 297$ eV, $E_1 > E_l$, the primary electrons reach S_2 and now stimulate, at a yield larger than 1, the production of secondary electrons with the energy T_S. These are accelerated by the electric field and produce a secondary current in the layer C_1. This current increases with E_0 as long as these secondary electrons are absorbed within C_1; then, it decreases when they can escape through S_0, as already explained.

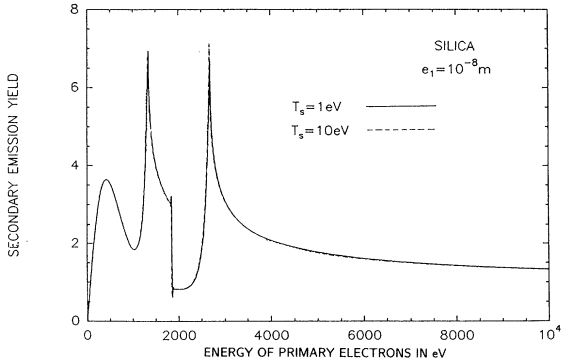

FIG. 3. Yield of secondary electron emission for silica versus the energy of the incident electron, for porous materials, depending on the temperature T_S characterizing the energy of the emitted electrons; $e_1 = 0.01$ μm.

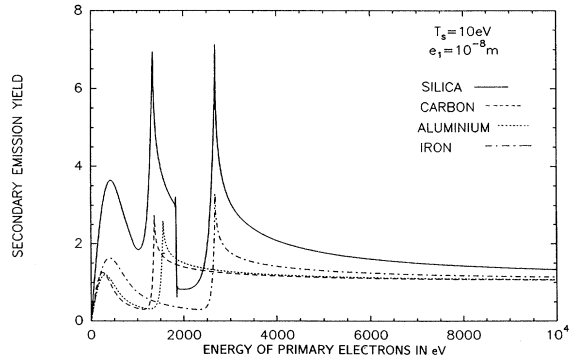

FIG. 5. Yield of secondary electron emission for silica, iron, carbon, and aluminum (Al_2O_3) versus the energy of the incident electron, for porous materials; $e_1 = 0.01$ μm.

The sharp end of the first peak coincides with the new state in which $E_1 = E_h - T_S$ (when $E_0 = 1629$ eV), for which the electric field in the pore no longer accelerates the secondary electrons in such a way that they reach S_1. At that point, the current from S_2 becomes zero and the secondary current is only due to the primary electrons in C_1. An increase of the energy decreases the production rate in C_1, so that the discrepancy is weakened when e_1 increases. For increased T_S the sharp end of the first peak appears for a lower energy since the case in which the field inside the pores accelerates the electrons is reached more quickly (Fig. 3)

For E_0 greater than 1629 eV, but lower than 1639 eV, for which $E_1 = E_h$, a reverse electric field appears; the secondary current from S_2 reaches S_1 though it is decelerated. Beyond this value the field accelerates the secondary electrons; the secondary current from S_2 is first completely absorbed within C_1; then it crosses C_1 for larger energies, generating the second peak.

In any case, as just explained, the separation of the two peaks is a consequence of the assumption of one unique velocity for the incident particles (monokinetic beam). This assumption, which at this step of the investigations allows detailed calculations with correct orders of magnitude and enables us to understand the physical phenomenon, can be removed, but this implies huger computations out of the scope of this paper (but envisaged for a forthcoming one). A distribution of velocities of incident particles, in other words a continuous spectrum of energies, would produce a superposition of yields with the same topology but shifted in energy, thus broadening the peaks and mixing them.

Figure 5 compares results for various materials under the same conditions. Figure 6 shows the difference of potential between the two faces of the pore versus the energy of the primary electrons under these conditions. It is noticeable that the strength of the FDSE field is fairly strong as soon as $E_0 > 1000$ eV for Si, C, and Al_2O_3, whereas $E_0 > 1700$ eV is necessary for F_e.

VII. CONCLUSION

The properties of this very simple model of porous material easily emphasize and illustrate the enhancement and the broadening in frequency of the yield of secondary-electron emission in a porous medium, due to the growth of strong electric fields in the vacuum pores because of the small sizes of these pores.

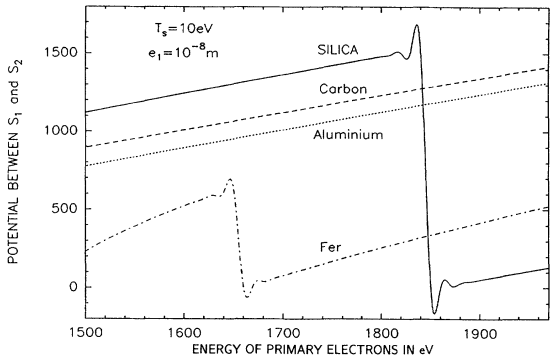

FIG. 6. Difference of potential between the surfaces S_1 and S_2 versus the energy E_0 of the incident electrons for silica, iron, carbon, and aluminum (Al_2O_3).

The enhancement is characterized by two emission peaks for small energies of the primary electrons and by an increase of the yield roughly by a factor of 4 for large energies. Of course, local variations of the pore size may shift, broaden, or mix the peaks, the final effect being a broadening of the yield profile in energy, just as can result from a complete distribution of energies for incident electrons.

Discussing the great interest of such a mechanism in astrophysics is out of the scope of the present paper, but we can already mention the importance of this mechanism for all processes involving interactions of solid materials with hot plasmas or highly energetic charged particles; for instance, in dust grain charge and dynamics. This also concerns the formation of complex molecules in cold media, for which both the rates of chemical reactions between molecules and their migration over the surface of solids can be accelerated by strong electric fields.

[1] H. Jacobs, J. Freely, and F. A. Brandt, Phys. Rev. **88**, 3, 492 (1952).
[2] J. M. Millet and J.-P. J. Lafon, in *Proceedings of the 18th International Conference on Phenomena in Ionized Gases, Swansea,* edited by N. T. Williams (Hilger, London, 1987), p. 232.
[3] J. M. Millet, J.-P. J. Lafon, and J. C. Gonin, Astron. Astrophys. **214**, 327 (1989).
[4] J. M. Millet, J.-P. J. Lafon, and E. Gunter, C. R. Acad. Sci. Ser. II **317**, 1185 (1993).
[5] J. R. Hill and D. A. Mendis, Moon Planets **21**, 3 (1979).
[6] R. H. Giese, K. Weiss, R. H. Zerull, and T. Ono, Astron. Astrophys. **95**, 265 (1978).
[7] K. G. McKay, Adv. Electron. Acad. Press **1**, 109 (1948).
[8] H. Jacobs, Phys. Rev. **84**, 5 (1951); **84**, 877 (1951).
[9] F. A. Brandt and H. Jacobs, Phys. Rev. **97**, 1 (1955); **97**, 81 (1955).
[10] P. Goldreich and W. R. Ward, Astrophys. J. **183**, 1051 (1973).
[11] J.-P. J. Lafon, Ph. Lamy, and J. M. Millet, Astron. Astrophys. **95**, 295 (1981).
[12] B. Feuerbacher, R. F. Willis, and B. Fitton, Astrophys. J. **181**, 101 (1972).
[13] R. Whiddington, Proc. R. Soc. London **35**, 300 (1912).
[14] N. Bohr, Philos. Mag. **25**, 10 (1913).
[15] N. Bohr, Philos. Mag. **30**, 381 (1915).
[16] J. R. Young, Phys. Rev. **103**, 292 (1957).
[17] B. T. Draine and E. E. Salpeter, Astrophys. J. **231**, 77 (1979).